Journal of Electromagnetic Waves and Applications

ISSN: 0920-5071 (Print) 1569-3937 (Online) Journal homepage: https://www.tandfonline.com/loi/tewa20

Impact of material characteristics on the general optical behavior of perforated surface plasmon system

Alireza Shabani, Neda Rahmani & Mehdi Khazaei Nezhad

To cite this article: Alireza Shabani, Neda Rahmani & Mehdi Khazaei Nezhad (2019): Impact of material characteristics on the general optical behavior of perforated surface plasmon system, Journal of Electromagnetic Waves and Applications, DOI: 10.1080/09205071.2019.1654931

To link to this article: https://doi.org/10.1080/09205071.2019.1654931

Published online: 20 Aug 2019.

JOURNAL OF ELECTROMAGNETIC WAVES AND APPLICATIONS
https://doi.org/10.1080/09205071.2019.1654931

Impact of material characteristics on the general optical behavior of perforated surface plasmon system

Alireza Shabani[a], Neda Rahmani[b] and Mehdi Khazaei Nezhad[a]

[a]Department of Physics, School of Science, Ferdowsi University of Mashhad, Mashhad, Iran; [b]Faculty of Physics, Shahrood University of Technology, Shahrood, Iran

ABSTRACT

In this paper, we studied the impact of material characteristics on the optical response of a perforated surface plasmon system as a general trend by employing dielectric function of metallic film. To this end, different artificial materials were modeled based on a single interband transition peak in the form of a Lorentzian function in the imaginary part of dielectric function ε_2 as well as a Drude term for free electron feature. The impact of place, strength and broadening of interband peak of metallic film were evaluated on the optical transmission spectrum. Our results revealed that these peaks affect the excited modes in the form of a decrease in the intensity of transmitted beam at corresponding frequencies. This decrease was proportional to the strength and width of the peak, and interpreted as an optical dissipation coming from material specifics. The present study provides a better insight into how the optical transmission response of such systems can be tuned for a particular goal or application using material characteristics.

ARTICLE HISTORY
Received 2 July 2019
Accepted 7 August 2019

KEYWORDS
Material characteristics; dielectric function; surface plasmon system; interband transmission; optical loss

Introduction

Studies about the optical behavior of perforated surface plasmon systems can be categorized into two main parts. First, the investigations that focus on seeking the relations between geometrical parameters, including hole dimension, lattice constant, thickness of metallic/dielectric layer, and excited surface plasmon modes of the system [1–5]. Second, the studies devoted to find new materials with improved optical properties to be employed in surface plasmon applications or replace conventional metals such as Au and Ag [6–10]. The proposed materials in such papers should have an acceptable optical quality factor for surface plasmon behavior [11–13], and simultaneously meet the particular conditions required for desired applications. These research studies are limited to a few known cases, such as ZrN, AZO, TiN, which were separately presented as some individual case studies. Thus, they are not able to provide a general view on how the material characteristics

CONTACT Alireza Shabani al.shabani@mail.um.ac.ir Department of Physics, School of Science, Ferdowsi University of Mashhad, Mashhad 9177948974, Iran

can affect the surface plasmon behavior. As a result, it can be said that the general relation between the material used in such systems and excited surface plasmon modes has remained unknown and more investigations are essential to be done in this field.

In this paper, we provide a comprehensive study to explore governing optical relations between the material property and the mesoscopic geometry. In fact, a general trend is sought during the paper by employing a surface plasmon system and focusing on optical transmission responses. Since all optical features of a material could be found in the dielectric function, we concentrate our studies on evaluating the impact of dielectric function on the optical transmission spectrum of a perforated surface plasmon system.

Dielectric function is known as the main quantity to describe the optical behavior of a material in solid state physics [14–16]. It is known as a fingerprint for different materials demonstrating their interaction with incident electromagnetic fields in the form of a response function for a wide range of energies or wavelengths [17–19]. The real part of dielectric function (ε_1) shows the ability of being electrically polarized, while the imaginary part of dielectric function (ε_2) denotes the optical loss in material [6]. In addition to the optical properties, the dielectric function provides other useful information such as the conductivity nature of a compound, including metal and insulator. This implies that in a metal there is an infinite value for ε_2 in energies near zero [20–22], attributed to free electrons effect, while an insulator or semiconductor has a finite value at zero energy (usually zero) due to the band gap [23–25]. The dielectric function is also used in sensing applications, where it exposes a shift in energy when an atom or molecule is absorbed on the surface of structure [26–28]. In spite of the numerous usage of dielectric function in the literature, which is representative of its importance in analyzing the optical behavior of materials, it seems to have potential for further investigations on its unknown aspects in the interdisciplinary fields, specifically, in solid state physics and optics.

In order to bridge the gap between material characteristics and geometry, we designed an unrealistic set-up in which the effect of dielectric function, as a common quantity between solid-state physics and optics, was investigated on the optical transmission behavior of a perforated surface plasmon configuration. In other words, the impact of a quantity that comes from atomic scale interactions was studied on the transmission spectrum of a known system with the mesoscopic scale.

To this end, an artificial dielectric function was selected in the form of a single Lorentzian peak for ε_2, which is representative of a series of electron interband transitions in a specific range of energies. This single peak is completely unrealistic as no matter could be found with this characteristic in the nature. It is interpreted as (i) an electron transition from occupied states to empty states around the Fermi energy from solid state physics view and (ii) an energy dissipation of an incident electromagnetic wave originated from the absorption and re-emission mechanism of light by electrons in any random directions from optics view. Subsequently, each proposed material (modeled Lorentzian peak) was used in the metallic film of perforated system in order to investigate the material effect.

We hope our results can pave the way for tuning the optical properties of the each arbitrary geometry by manipulating the optical characteristics of constituent materials. It is possible, for instance, by employing engineering methods, such as doping guest atoms into a compound in order to modify or improve the optical properties. Such a study was performed in our previous work where the transmission behavior of a perforated surface plasmon of Au-doped TiN was investigated as a function of Au concentration by using

a combination of Density functional theory and finite-difference time-domain method (FDTD) method [29]. It was observed that the doping process affects the electronic features of the compound such as density of states through atomic scale interactions which directly influences the optical dielectric function and consequently, transmission spectrum behavior.

This paper is organized in four sections. The second section is devoted to computational parameters used in the simulations. In the third section, the main aim of this research, including interpretation and analysis, is discussed, and all obtained results are summarized in the last section.

Optical simulation

The Optiwave package was employed to simulate our proposed geometry containing a metallic thin film on the top of a dielectric substrate. As shown in Figure 1, a periodic array of square holes were placed within the metallic film in which the distance between two successive holes was the same and equal to the 250 nm for both *x*- and *y*-directions. Other structural parameters including size of holes, thickness of metallic film and dielectric layer were 150, 20 and 50 nm, respectively. After full convergence calculations, a mesh parameter 5 nm was selected along the *x*-, *y*- and *z*-directions and the system was irradiated by a Gaussian modulated continuous electromagnetic wave with time offset 4e-15 s and half width 0.8e-15 s which propagated along the *z*-direction and linearly polarized in the *x*-axis direction (as shown in Figure 1). Since the simulated geometry lies in the *x*–*y* plane, the periodic boundary condition was used for the *x*- and *y*-directions and absorbing perfectly matched layer for the *z*-direction. The Optiwave package uses FDTD to solve Maxwell equations for electromagnetic waves through discretizing them by means of the fundamental definition of derivative equation [30]. By using this method, temporal and spatial dependencies of electric and magnetic fields are found at any point of the simulated geometry [31]. Finally, the calculated time-dependence electromagnetic fields are converted to the frequency- dependence quantities by means of Fourier transforms.

In order to generate our artificial materials with different optical characteristics, we employed Lorentzian function distributions with bell shape in ε_2, given by Equation (1), indicating a series of electron interband transitions.

$$f(x; x_c, \gamma, I) = \frac{2I}{\pi} \frac{\gamma}{4(x - x_c)^2 + \gamma^2}; \tag{1}$$

Here x_c is the location of distribution center, while γ specifies the full width of function in half the maximum height and *I* shows the height of peak.

Subsequently, to extract optical parameters required for the simulation of modeled materials in the proposed configuration via the Optiwave package, the Drude–Lorentz model was used with only two terms in ε_2. This model includes the effects of free-electrons as well as a particular range of interband transitions, which is given by Equation (2):

$$\varepsilon(\omega) = \varepsilon_\infty(\omega) + \sum_{j=0}^{1} \frac{f_j \omega_p^2}{(\omega_j^2 - \omega^2) - i\omega\gamma_j}; \tag{2}$$

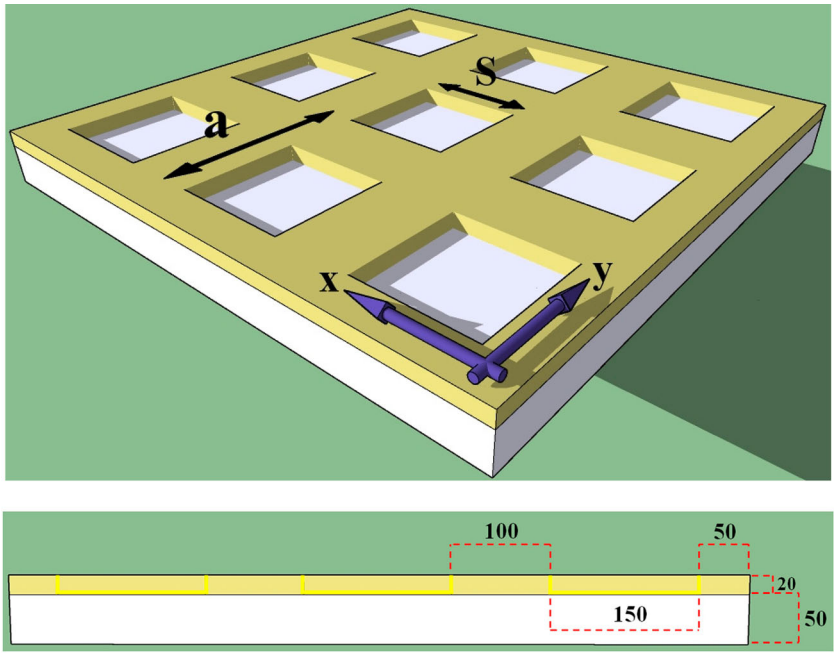

Figure 1. Schematic view of a perforated surface plasmon system (top panel) consisting of a square array of subwavelength air holes introduced into a dielectric layer. The periodic lattice constant and size of hole are shown by a and S, respectively. Cross-sectional view (bottom panel) containing geometrical parameters values used in the simulations. All values are in the nanometer scale.

where ω_j, γ_j and f_j are oscillator resonance frequencies, bandwidths and oscillator strengths, respectively. The background permittivity is described by ε_∞ and ω_p is the plasma frequency. We set $\varepsilon_\infty = 1$ and $\omega_p = 13.67 \times 10^{16}$ Rad/s in all simulations [32].

Results and discussion

At first, we investigated the transmission behavior of the perforated surface plasmon system with respect to the metallic film replaced by different materials with difference only in the place of resonance peak in ε_2. The resonance frequency changed from 1.5 to 2.5×10^{15} Rad/s, while other parameters such as the height and width of peaks were kept constant. Since each individual peak is in the form of a Lorentzian function, we can easily extract those parameters required for defining our unrealistic material into the Optiwave simulating package by comparing Lorentzian function parameters and the optical quantities of ε_2.

The corresponding physical quantities for each material (three peaks in Figure 2), including resonance frequency, strength and damping coefficient, are listed in Table 1. By irradiating of the proposed two-dimensional system, containing periodically a perforated unrealistic metallic film and a dielectric layer, one can see that some peak and dips appeared within transmission spectrum (shown in Figure 2(b)) [33,34], which show different orders of excited surface plasmon modes in a perforated surface plasmon system. In addition, the

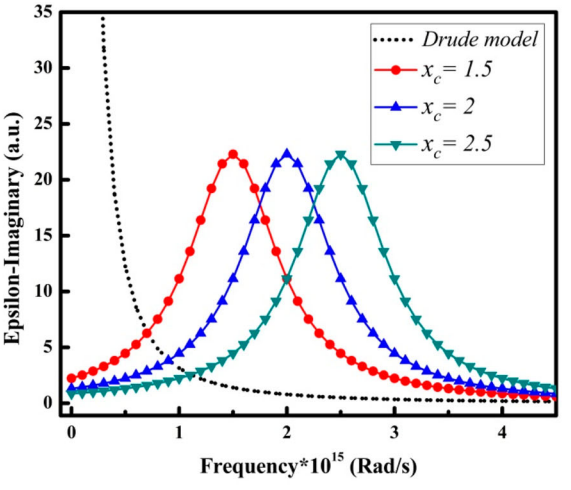

(a)

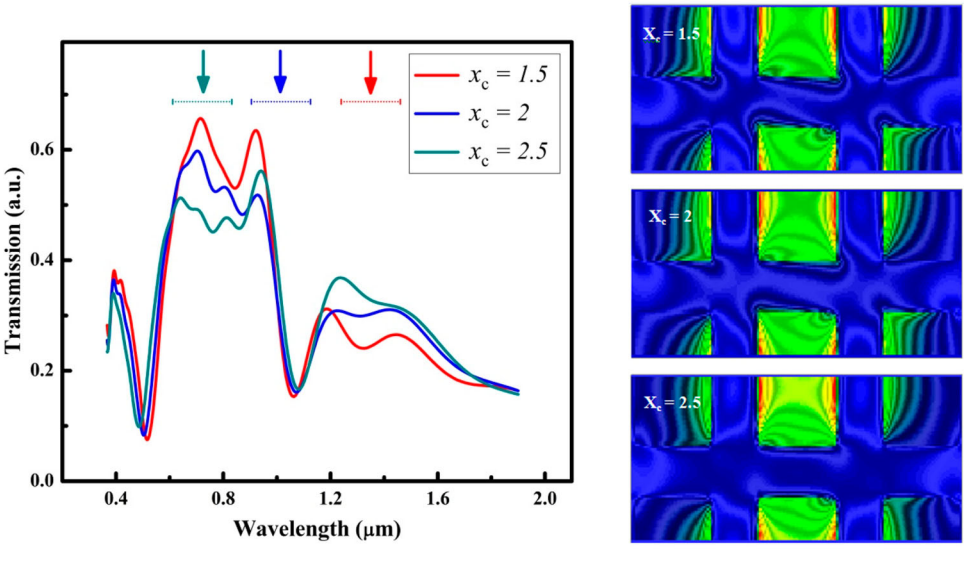

(b) (c)

Figure 2. (a) Imaginary part of dielectric function for three proposed materials based on Table 1. Each individual peak is representative of a resonance and indicator of a specific material. The Drude term is the same for three materials. (b) Optical transmission spectrum of a perforated surface plasmon system with respect to different modeled materials as a metallic film. (c) The amplitude of Pointing vector in the *z*-direction (Sz) at metal–dielectric interface for the materials at the wavelength of $\lambda = 753$ nm.

broad peak with highest intensity is the main characteristic of such a metal–dielectric system which is known as an extraordinary optical transmission (EOT) peak [35,36]. It is seen that the same order of excited modes in all three materials occurred approximately in the same wavelength. A small difference in the place of identical peaks can be explained by equation $\lambda_{sp} = \frac{a}{\sqrt{n^2+m^2}}\sqrt{\frac{\varepsilon_d\varepsilon_m}{\varepsilon_d+\varepsilon_m}}$, which shows the relation between wavelength of excited

Table 1. The Lorentzian peaks parameters for three proposed materials including f, γ and $\boldsymbol{x_c}$ and corresponding Drude–Lorentz quantities for dielectric function comprising resonance frequencies, oscillation strength and damping coefficient.

Material	ω_r(10^{15} Rad/s)	γ (10^{15} Rad/s)	f	ω_p(10^{15} Rad/s)
Drude term	0	0.2	1	13.673
$f = 30, \gamma = 1, x_c = 1.5$	1.5	1	0.153315	13.673
$f = 30, \gamma = 1, x_c = 2$	2	1	0.2043	13.673
$f = 30, \gamma = 1, x_c = 2.5$	2.5	1	0.255525	13.673

Notes: The difference between materials is only in the resonances frequencies. The Drude term is the same for all materials.

modes, geometrical parameter and material's quantities [37,38]. It implies that changes of the dielectric function of metallic film in such system will result in a slight shift in the wavelength of excited surface plasmon modes.

It was reported in our previous study that the place of these modes only depends on the lattice constant of the structure [39], as this expression is in agreement with the aforementioned equation. Here, we fixed all geometrical parameters which also include the lattice constant, because our intention is just to evaluate the effect of dielectric function (material in used). By comparing transmission spectrum with the imaginary part of dielectric function ε_2, it is found that at frequencies which we have a resonance peak in ε_2, there is a significant decrease in the transmission spectrum for corresponding wavelengths. It is clear from Figure 2(b) that the lowest value for $x_c = 1.5$ material compared to two other cases occurs around $\lambda = 1255$ nm (red arrow) which is due to the peak in ε_2 at the frequency of $\omega = 1.5 \times 10^{15}$ Rad/s. In addition, the transmission spectrum of $x_c = 2$ material has the lowest value around EOT peak which corresponds to the peak at $\omega = 2 \times 10^{15}$ in ε_2, while for the material with a peak at $\omega = 2.5 \times 10^{15}$ in ε_2 the transmission spectrum has the lowest value around $\lambda = 753$ nm (dark cyan arrow). It can be concluded from above that wherever we have a peak in ε_2, a decrease in transmission spectrum will be expected at the corresponding region.

There are several phenomena in such a structure that affect the intensity of excited modes. First, surface plasmon polariton effect which occurs at metal–dielectric interface due to coupling between propagating component of electromagnetic field and free electron sea accumulated at the interface [40,41]. Second, localized surface plasmon resonance (LSPR), which is known as a collective movement and same phase oscillation of free electrons at sharp edges and tips of metallic film, originated from the action of mimicking incident electric field by electrons [42]. This phenomenon is limited to the nanometer scale of holes and it is responsible for hotspots in the field distribution pattern because of the irradiating nature of oscillating electrons. It was shown that more LSPRs lead to stronger hotspots that finally enhance transmission intensity [43]. Third phenomenon is related to the mechanism in which electromagnetic waves directly pass through the holes with minimum interaction with geometry which results in an improvement in transmission spectrum. This is called waveguide mode effect which is a characteristic of surface plasmon systems with subwavelength holes [44]. Moreover, there is a coupling between LSPRs at sharp edges and tips that could strongly affect the optical behavior of the system [40].

In order to confirm previous discussion and show the impact of chosen materials on the mentioned optical phenomena of the system, z-direction component of transmission power calculated by FDTD modeling was depicted for three supposed materials at the

wavelength of $\lambda = 753$ nm. Figure 2(c) shows the S_z distribution pattern for each material in a separate window, which includes a region with six square holes. The LSPRs at edges and corners of holes, waveguide mode within the central hole and LSPR interaction in the form of contour lines in the metallic region between holes, are clearly observed. It is found that hotspots for $x_c = 2.5$ case have the lowest brightness in comparison with $x_c = 1.5$ and 2 materials, which is representative of the weakest LSPR; therefore, the lowest enhanced local field. In contrast, the $x_c = 1.5$ material not only has the highest brightness and the largest size of hotspot but also shows the most relative LSPR interaction between hotspots due to high-contrast contour lines on the metallic film. All the aforementioned phenomena indicate more enhancement for transmission intensity of $x_c = 1.5$ material at $\lambda = 753$ nm compared to two other cases, which is in agreement with the calculated optical transmission spectrum in Figure 2(b). Since the single resonance peak in $\varepsilon_2$for the case of $x_c = 1.5$ (red arrow) is far enough from the discussed area around $\lambda = 753$ nm, the $x_c = 1.5$ material faces the least reduction in transmission intensity compared to two other cases. The similar discussion can be considered for two other regions of transmission spectrum in Figure 2.

It can be concluded that the electron interband transitions are responsible for the optical loss observed in the simulation as they play an important role in the energy dissipation of incident electromagnetic waves. By considering the band structure view in solid state physics, the incident beam can be absorbed by electrons in occupied states below the Fermi energy which causes their transition to unoccupied states. The excited electrons return to the lower energy states by emitting electromagnetic wave in the spatially random directions. This phenomenon causes fewer beams to reach to the observation area behind the structure which measures the transmission spectrum of the electromagnetic wave, thus there would be less intensity for the transmitted beam in the specific range of frequencies or wavelengths.

The obtained results show that the optical behavior of such geometry is strongly dependent on the material used in the system and imply a general trend, exhibiting a competition between material and geometry in controlling optical characteristics of the system. This provides a clear insight into how the optical properties can be tailored for a specific purpose or particular application. For instance, regarding the sensing application by utilizing perforated surface plasmon system, having a sharp and distinct EOT peak is highly demanded. It implies that if we could find a material with two interband transition peaks in ε_2 at frequencies of $\omega = 1.5$ and 2.5×10^{15} Rad/s, one can expect a sharp and distinct EOT peak, proper for sensing applications.

In the next section, the impact of peak strength in ε_2 was chased on the excited plasmon modes of transmission spectrum. In this unrealistic case, we introduced seven different materials with only one resonance at the frequency of 2×10^{15} Rad/s in which all materials have the same plasmon frequency and damping factor but different in the resonance strength, originated from various heights of Lorentzian peak. In order to do that, we considered different values for *I* parameter in Lorentzian function ranging from 1 to 30, given by Table 2. Moreover, the Drude model used in the previous simulations was employed here to provide metallic behavior with the characteristic of the Electron Sea. It should be noted again that the final amounts of ε_2 for a material are obtained by the summation of Drude model and related Lorentzian distribution. In fact, each peak is attributed to a new material in which the difference in optical behavior of these materials stems only from their resonance intensity in the given frequency.

Table 2. The Lorentzian peaks parameters for the proposed materials including l, γ and $\boldsymbol{x_c}$ and corresponding Drude–Lorentz quantities for dielectric function comprising resonance frequencies, oscillation strength and damping coefficient.

Material	$\boldsymbol{\omega_r}$(10^{15} Rad/s)	γ (10^{15} Rad/s)	f	$\boldsymbol{\omega_p}$(10^{15} Rad/s)
Drude term	0	0.2	1	13.673
$l = 1, \gamma = 1, x_c = 2$	2	1	0.00681	13.673
$l = 5, \gamma = 1, x_c = 2$	2	1	0.03405	13.673
$l = 10, \gamma = 1, x_c = 2$	2	1	0.0681	13.673
$l = 15, \gamma = 1, x_c = 2$	2	1	0.10215	13.673
$l = 20, \gamma = 1, x_c = 2$	2	1	0.1362	13.673
$l = 25, \gamma = 1, x_c = 2$	2	1	0.17025	13.673
$l = 30, \gamma = 1, x_c = 2$	2	1	0.2043	13.673

Notes: The difference between materials is only in the oscillation strength. The Drude term is the same for all materials.

The Drude–Lorentz model was used to extract the optical parameters required for defining our proposed materials into the Optiwave package for FDTD simulations. The results are listed in Table 2. It is seen that ω_r, γ and ω_p are the same for all peaks while f_j, which is known as oscillator strength, is different. We replaced the metallic film of dielectric–metal configuration with these unrealistic materials in order to see the impact of f_j parameter on the optical behavior of the simulated geometry.

As it is clear from Figure 3(b), since all materials have only one resonance around $\omega = 2 \times 10^{15}$ Rad/s, it is expected that all changes occur around the EOT peak. One can see that the material with $l = 1$, which corresponds to the smallest peak in ε_2, has the most optical transmission at EOT peak, while by increasing l, the intensity of transmitted beam gradually decreases as it reaches to the lowest amount for $l = 30$. For $l = 30$ material, the peaks showing excited surface plasmon modes have the lowest sharpness and contrast compared to $l = 1$ and 5 even the EOT peak disappeared for this material. It is completely in agreement with our previous explanation about relation between ε_2 and optical loss of system: increasing the peak height of a resonance in ε_2, intensifies the energy dissipation at corresponding frequencies which leads to the less intensity of transmitted beam.

Figure 3(c) demonstrates S_z distribution calculated by FDTD simulations for $l = 1, 10, 20$ and 30. It is seen that there is more intensity for $l = 1$ at sharp edges and tips in comparison with others which is presumably due to the more excited LSPRs and consequently, stronger hotspots and enhanced local fields. Moreover, there are more contour lines between square holes for $l = 1$ case which are indicators of more interaction between LSPRs, resulting in a growth in the intensity of transmitted beam for the lowest value of l parameter. This trend confirms the behavior observed in the optical transmission spectrum of Figure 2(b).

In the following, we evaluated the effect of broadening of interband transmission peak on the optical behavior of the proposed mesoscopic system. For this reason, four unrealistic materials were suggested with only one resonance at $\omega = 2 \times 10^{15}$ Rad/s in the form of a Lorentzian peak in ε_2, while γ parameter varied from 0.4 to 1 (see Figure 4(a)). For all materials the peaks height and plasmon frequency were the same. Similar to the previous simulations, metallic behavior was included to the materials by adding the Drude term into the imaginary part of dielectric function in order to expect the surface plasmon phenomena.

According to Table 3, all materials in this section have the same optical quantities expect the γ parameter which is approximately equal to the full width in half maximum of an interband transition peak. It is also known as a damping coefficient of resonance and associated

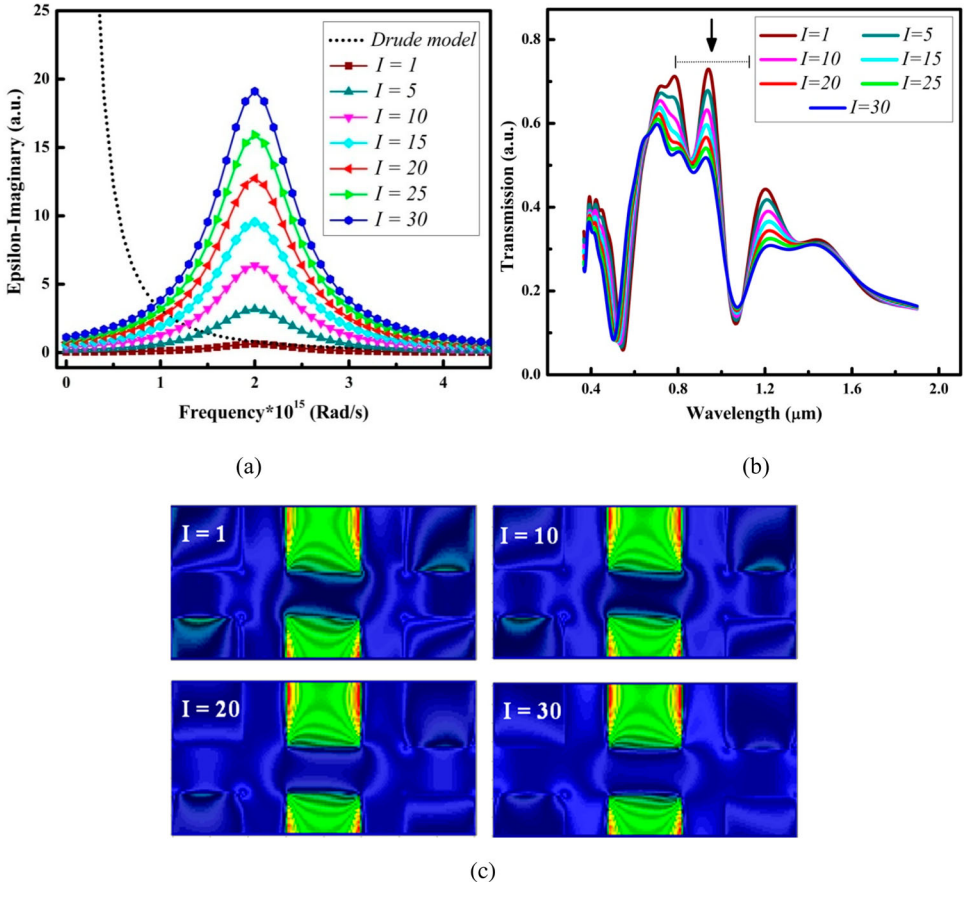

Figure 3. (a) Imaginary part of dielectric function for different unrealistic materials introduced in Table 2. The Drude term is the same for all materials. (b) Optical transmission spectrum of a perforated surface plasmon system with respect to different modeled materials as the metallic film. (c) The amplitude of Pointing vector in the *z*-direction (Sz) at metal–dielectric interface for the selected materials at the wavelength of $\lambda = 941$ nm (EOT peak).

with the relaxation time of an excited state [45]. By replacing the metallic film of surface plasmon configuration with the proposed materials, one can see from Figure 4(b) a higher relative transmission intensity around the EOT peak for the $\gamma = 0.4$ material compared to other three cases. It is also observed that by approaching to the center of resonance, the difference in transmission intensity of model materials decreases because all four materials have the same peak strength in the imaginary part of dielectric function ε_2 (Figure 4(a)). The obtained behavior implies that the γ parameter is directly related to the effectiveness and coverage range of a resonance peak in decreasing the intensity of transmitted beam. It means those materials with smaller damping factor have a shorter coverage range for influencing on the system via decreasing the optical intensity, as it is seen for $\gamma = 0.4$. In contrast, materials with larger γ decline the transmission intensity of electromagnetic wave in a wider spectrum because of their more coverage range, as observed for the $\gamma = 1$ case. In

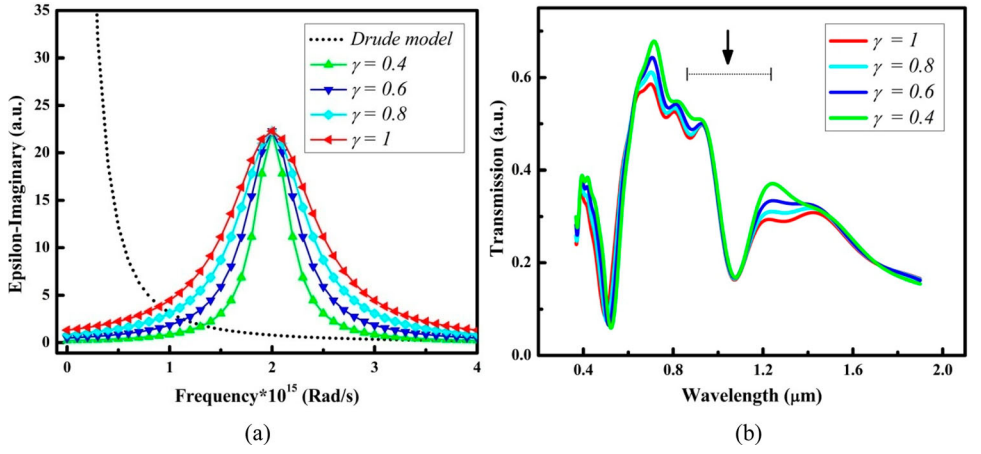

Figure 4. (a) Imaginary part of dielectric function for different unrealistic materials with various damping factors of resonance based on Table 3. The Drude term is the same for all materials. (b) Optical transmission spectrum of a perforated surface plasmon system with respect to different modeled materials as the metallic film.

Table 3. The Lorentzian peak parameters for the proposed materials including I, γ and $\boldsymbol{x_c}$ and the corresponding Drude–Lorentz quantities for dielectric function comprising resonance frequencies, oscillation strength and damping coefficient.

Material	$\boldsymbol{\omega_r}$(10^{15} Rad/s)	γ (10^{15} Rad/s)	f	$\boldsymbol{\omega_p}$(10^{15} Rad/s)
Drude term	0	0.2	1	13.673
$I = 14, \gamma = 0.4, x_c = 2$	2	0.4	0.095	13.673
$I = 21, \gamma = 0.6, x_c = 2$	2	0.6	0.143	13.673
$I = 28, \gamma = 0.8, x_c = 2$	2	0.8	0.190	13.673
$I = 35, \gamma = 1, x_c = 2$	2	1	0.238	13.673

Notes: The difference between materials is only in the damping coefficient of resonance. The Drude term is the same for all materials.

other words, by increasing γ parameter, the optical loss becomes active in a broader range and causes the decreased intensity to occur in a more extended region.

The mentioned discussion shows the role of γ parameter in controlling the optical behavior of a system and as it is clear from its name, the damping coefficient is a factor showing the rang of optical loss. It is worth mentioning that the usage of optical loss term completely depends on the research aim and application which is intended to be done. For instance, in the present study, one expects to have a material with the maximum of transmission spectrum stems from surface plasmon phenomena while according to the nature of interband transitions which is based on the absorption and randomly spatial re-emission mechanism of incident electromagnetic wave, using the term of optical loss seems to be meaningful in this case. In contrast, there are particular applications in which the absorption process plays a vital role in the performance and efficiency of those application such as light emitting diode (LED) and solar cell devices, which require materials with high absorption rate in particular ranges of frequencies. This indicates that applying the term of optical loss, caused by interband transitions, would be meaningless in such cases.

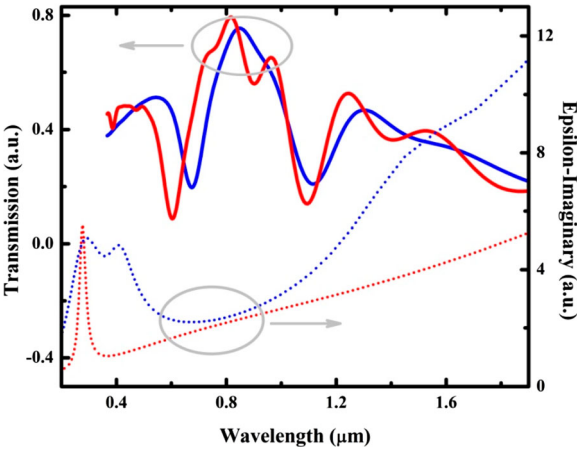

Figure 5. Optical transmission spectrum of perforated surface plasmon system (top) containing Au (solid blue line) and Ag (solid red line) as the metallic film, and reproduced imaginary part of dielectric function ε_2 (bottom) for Au (dotted blue line) and Ag (dotted red line).

In order to confirm the previous results and evaluate the validity of our discussion for real materials, we calculated the optical transmission spectrum of a perforated surface plasmon system for two known metals: gold and silver. To this end, we employed default values of the imaginary part of dielectric functions ε_2 embedded in the Optiwave package, which were taken from Ref. 32 and obtained based on the experimental studies. In the following, the imaginary parts of dielectric function of Au and Ag were retrieved by employing the method used in prior sections except that the process was completely reversed as we had some known physical quantities for ε_2 and needed to plot them by modeling corresponding Lorentzian functions.

In Figure 5, we depicted both optical transmission spectrum of a perforated surface plasmon system containing Au and Ag as metallic film and reproduced imaginary part of dielectric function in order to seek the effect of material characteristics. Different excited modes are observed for both cases which are due to the nature of such geometry in coupling the propagating in-plane component of incident electromagnetic wave and orderly subwavelength holes.

The surface plasmon modes for both metals are approximately excited at the same wavelengths. It is because of a relatively close value for plasma frequency of Au and Ag: $\omega_{p\mathrm{Au}} = 13.69 \times 10^{15}$ and $\omega_{p\mathrm{Ag}} = 13.67 \times 10^{15}$ Rad/s. Moreover, it is seen that Ag has more transmission intensity than Au in most wavelengths, especially at the place of excited peaks. The obtained results are completely consistent with our previous discussion, indicating that more imaginary part of dielectric function leads to the less transmission spectrum. By comparing two plots in the bottom of Figure 5, it is observed that Au has relatively greater dielectric function than Ag in entire wavelengths which results in more optical loss, and therefore less transmission intensity for that. A greater damping coefficient for Au at resonance with zero energy (Drude peak) as well as lower-energy excited interband transition peaks, which appear in Vis-IR window compared to UV peaks of Ag, makes a larger imaginary part of dielectric function for that. Furthermore, it should be noted that since there is a small difference in the imaginary part of dielectric function for Au and Ag, it is expected

that the optical transmission intensity has also a slight difference at excited peaks, as it was observed for the modeled unrealistic materials in Figure 3(b) that a 60% increase in the imaginary part of dielectric function between $I = 15$ and 25 led to a 9% decrease in transmission spectrum.

Conclusion

In this paper, we sought a general trend between material characteristic and optical behavior of a mesoscopic system. We presented our study in the framework of an example for optical transmission spectrum of a perforated surface plasmon configuration with respect to various unrealistic and artificial materials modeled as metallic film. The optical characteristic of the proposed metallic materials were demonstrated in the imaginary part of dielectric function which included a single interband transition peak with Lorentzian distribution (different place, height and width of resonance) as well as a Drude term for metallic behavior. It was revealed that the optical transmission response of such a structure was influenced by two effects. First, different excited modes of surface plasmon at metal–dielectric interface appeared as separate peaks and dips, and second, optical loss in the form of a decrease in transmission spectrum originated from interband transition peaks in the imaginary part of dielectric function. This decrease was proportional to the height, width and place of resonance peak. The same simulations were done for some realistic materials including Ag and Au that confirmed the obtained results. This study provided a comprehensive view on how material characteristics control general optical behavior of a mesoscopic system and showed the importance of material selection for particular goals and applications.

Disclosure statement

No potential conflict of interest was reported by the authors.

Notes on contributors

Alireza Shabani received the PhD degree in solid state physics from the Ferdowsi University of Mashhad, Iran, in 2018 and currently is a researcher at FUM. His research interests include plasmonics and metamaterials by using computational methods such as DFT and FDTD.

Neda Rahmani received the MSc degree in solid state physics from the Ferdowsi University of Mashhad, Iran, in 2012 and currently is a PhD candidate in solid state physics at Shahrood University of Technology. Her research interests include multiferroic materials using first principle calculations.

Mehdi Khazaei Nezhad received his MSc and PhD degrees in physics from Sharif University of Technology on 2012 and 2014, respectively. Then he joint as a faculty member to physics department in Ferdowsi University of Mashhad, Iran from January 2015.

References

[1] Popov E, Enoch S, Bonod N. Absorption of light by extremely shallow metallic gratings: metamaterial behavior. Opt Express. 2009;17:6770–6781.

[2] Ruan Z, Qiu M. Enhanced transmission through periodic arrays of subwavelength holes: the role of localized waveguide resonances. Phys Rev Lett. 2006;96:233901.

[3] Zhang X, Liu G, Hu Y, et al. Enhanced optical transmission in a plasmonic nanostructure perforated with compound holes and nanorods. Opt Commun. 2014;325:105–110.
[4] Li WD, Hu J, Chou SY. Extraordinary light transmission through opaque thin metal film with subwavelength holes blocked by metal disks. Opt Express. 2011;19:21098–21108.
[5] Behera G, Ramakrishna SA. Tri-layered composite plasmonic structure with a nanohole array for multiband enhanced absorption at visible to NIR frequencies: plasmonic and metamaterial resonances. J Phys D Appl Phys. 2016;49:075103.
[6] Naik GV, Shalaev VM, Boltasseva A. Alternative plasmonic materials: beyond gold and silver. Adv Mater. 2013;25:3264–3294.
[7] Lin JY, Zhong KD, Lee PT. Plasmonic behaviors of metallic AZO thin film and AZO nanodisk array. Opt Express. 2016;24:5125–5135.
[8] Naik GV, Kim J, Boltasseva A. Oxides and nitrides as alternative plasmonic materials in the optical range. Opt Mater Express. 2011;1:1090–1099.
[9] Naik GV, Schroeder JL, Ni X, et al. Titanium nitride as a plasmonic material for visible and near-infrared wavelengths. Opt Mater Express. 2012;2:478–489.
[10] Kesim YE, Battal E, Okyay AK. Plasmonic materials based on ZnO films and their potential for developing broadband middle-infrared absorbers. AIP Adv. 2014;4:077106.
[11] Kumar M, Ishii S, Umezawa N, et al. Band engineering of ternary metal nitride system $Ti_{1-x}Zr_xN$ for plasmonic applications. Opt Mater Express. 2016;6:29–38.
[12] West PR, Ishii S, Naik GV, et al. Searching for better plasmonic materials. Laser Photon Rev. 2010;4:795–808.
[13] Guler U, Naik GV, Boltasseva A, et al. Performance analysis of nitride alternative plasmonic materials for localized surface plasmon applications. Appl Phys B. 2012;107:285–291.
[14] Djurišić AB, Li EH. Dielectric function models for describing the optical properties of hexagonal GaN. J Appl Phys. 2001;89:273–282.
[15] Olmon RL, Slovick B, Johnson TW, et al. Optical dielectric function of gold. Phys Rev B. 2012;86:235147.
[16] Dresselhaus MS. Solid state physics part ii optical properties of solids. 2001.
[17] Kasap SO. Principles of electronic materials and devices. New York: McGraw-Hill; 2006.
[18] Li Y. Plasmonic optics: theory and applications. Bellingham: SPIE Press; 2017.
[19] Hao F, Nordlander P. Efficient dielectric function for FDTD simulation of the optical properties of silver and gold nanoparticles. Chem Phys Lett. 2007;446:115–118.
[20] Ehrenreich H, Philipp HR, Segall B. Optical properties of aluminum. Phys Rev. 1963;132:1918.
[21] Patsalas P, Kalfagiannis N, Kassavetis S. Optical properties and plasmonic performance of titanium nitride. Materials (Basel). 2015;8:3128–3154.
[22] Rioux D, Vallières S, Besner S, et al. An analytic model for the dielectric function of Au, Ag, and their alloys. Adv Opt Mater. 2014;2:176–182.
[23] Song TT, Yang M, Chai JW, et al. The stability of aluminium oxide monolayer and its interface with two-dimensional materials. Sci Rep. 2016;6:29221.
[24] Yu Y, Yu Y, Cai Y, et al. Exciton-dominated dielectric function of atomically thin MoS 2 films. Sci Rep. 2015;5:16996.
[25] Wang H, Zheng Y, Cai MQ, et al. First-principles study on the electronic and optical properties of BiFeO3. Solid State Commun. 2009;149:641–644.
[26] Huang X, Leng T, Georgiou T, et al. Graphene oxide dielectric permittivity at GHz and its applications for wireless humidity sensing. Sci Rep. 2018;8:43.
[27] Azimirad R, Safa S, Bayani AH. CO gas opto-electronic sensor using semiconductor graphene nanoribbons: a first-principles study. Phys Status Solidi (b). 2016;253:559–565.
[28] Jean-Mistral C, Sylvestre A, Basrour S, et al. Dielectric properties of polyacrylate thick films used in sensors and actuators. Smart Mater Struct. 2010;19:075019.
[29] Shabani A, Nezhad MK, Rahmani N, et al. Optical properties of Au-doped titanium nitride nanostructures: a Connection between density functional theory and finite-difference time-domain method. Plasmonics. 2019: 1–9. DOI:10.1007/s11468-019-00982-1.

[30] Yee K. Numerical solution of initial boundary value problems involving Maxwell's equations in isotropic media. IEEE Trans Antennas Propag. 1966;14:302–307.
[31] Taflove A, Hagness SC. Computational electrodynamics: the finite-difference time-domain method. Norwood: Artech house; 2005.
[32] Rakić AD, Djurišić AB, Elazar JM, et al. Optical properties of metallic films for vertical-cavity optoelectronic devices. Appl Opt. 1998;37:5271–5283.
[33] Behera G, Ramakrishna SA. Enhanced broadband transmission through structured plasmonic thin films for transparent electrodes. J Nanophotonics. 2014;8:083889.
[34] Liu JQ, He MD, Zhai X, et al. Tailoring optical transmission via the arrangement of compound subwavelength hole arrays. Opt Express. 2009;17:1859–1864.
[35] Liu Z, Liu G, Liu X, et al. Continuous copper film structures with broadband optical transparency. Mater Lett. 2015;139:12–14.
[36] Liu Z, Hang J, Chen J, et al. Optical transmission of corrugated metal films on a two-dimensional hetero-colloidal crystal. Opt Express. 2012;20:9215–9225.
[37] Braun J, Gompf B, Kobiela G, et al. How holes can obscure the view: suppressed transmission through an ultrathin metal film by a subwavelength hole array. Phys Rev Lett. 2009;103:203901.
[38] Weiner J. The physics of light transmission through subwavelength apertures and aperture arrays. Rep Progr Phys. 2009;72:064401.
[39] Shabani A, Roknabadi MR, Behdani M, et al. Extraordinary optical transmission of periodic array of subwavelength holes within titanium nitride thin film. J Nanophotonics. 2017;11:036006.
[40] Zhang X, Liu G, Liu Z, et al. Near-field plasmon effects in extraordinary optical transmission through periodic triangular hole arrays. Opt Eng. 2014;53:107108.
[41] Zhang X, Liu G, Hu Y, et al. Tunable extraordinary optical transmission in a metal film perforated with two-level subwavelength cylindrical holes. Plasmonics. 2014;9:1149–1153.
[42] Jin EX, Xu X. Plasmonic effects in near-field optical transmission enhancement through a single bowtie-shaped aperture. Appl Phys B. 2006;84:3–9.
[43] Wang Y, Qin Y, Zhang Z. Extraordinary optical transmission property of X-shaped plasmonic nanohole arrays. Plasmonics. 2014;9:203–207.
[44] Pendry JB, Martin-Moreno L, Garcia-Vidal FJ. Mimicking surface plasmons with structured surfaces. Science. 2004;305:847–848.
[45] Khurgin JB. Replacing noble metals with alternative materials in plasmonics and metamaterials: how good an idea? Philos Trans R Soc A Math Phys Eng Sci. 2017;375:20160068.